

## A QUIET DAY EMPIRICAL MODEL OF ELECTRON DENSITY IN THE INDIAN EQUATORIAL F-REGION

## ЭМПИРИЧЕСКАЯ МОДЕЛЬ ЭЛЕКТРОННОЙ ПЛОТНОСТИ В УСЛОВИЯХ НИЗКОЙ ГЕОМАГНИТНОЙ АКТИВНОСТИ В ИНДИЙСКОЙ ЭКВАТОРИАЛЬНОЙ F-ОБЛАСТИ

**M. Chamua**

*Tinsukia College, Department of Physics,  
Assam, India, mchamua@gmail.com*

**P.K. Bhuyan**

*Dibrugarh University, Department of Physics,  
Assam, India, pkbhuyan@gmail.com*

**K. Bhuyan**

*Dibrugarh University, Department of Physics,  
Assam, India, kalyanbhuyan@gmail.com*

**М. Чхамуа**

*Колледж Тинсукия, факультет физики,  
Ассам, Индия, mchamua@gmail.com*

**П.К. Бхуян**

*Университет Дибругарх, факультет физики,  
Ассам, Индия, pkbhuyan@gmail.com*

**К. Бхуян**

*Университет Дибругарх, факультет физики,  
Ассам, Индия, kalyanbhuyan@gmail.com*

**Abstract.** In this paper, we present a quiet day empirical model of electron density ( $N_e$ ) for the Indian equatorial zone at an altitude of 500 km. The model is applicable to all levels of solar activity and is based on the observation that the electron density in the F-region of the Indian zone is correlated with the  $F10.7$  cm solar flux at each local time and in every month. Using this characteristic, we describe the model for electron density. In this model, we have used the least square fit and the polynomial fit. The electron density measured by the Retarding Potential Analyzer (RPA) on board the SROSS C2 satellite from 1995 to 2000 and FORMOSAT-1 (ROCSAT-1) satellite, operated by the National Space Organization (NSPO, now the Taiwan Space Agency (TASA)) of the Republic of China (Taiwan), from 1999 to 2004 is used to derive the relationship between  $N_e$  and  $F10.7$ . The average altitudes of SROSS-C2 and FORMOSAT-1 are 500 km and 600 km respectively. Due to this height difference, the observed data obtained by FORMOSAT-1 is normalized to match the SROSS-C2 data. The model is compared with the observations and is found to be in good agreement with them. It is applicable to quiet ( $A_p < 15$ ) conditions and is limited to a fixed altitude of 500 km within the latitude range of  $10^\circ$  S to  $10^\circ$  N around the  $75^\circ$  E meridian.

**Keywords:** equatorial ionosphere; modeling; solar activity cycle; mathematical and numerical techniques.

**Аннотация.** В статье представлена эмпирическая модель электронной плотности ( $N_e$ ) в условиях низкой геомагнитной активности для индийской экваториальной зоны на высоте 500 км. Данная модель применима ко всем уровням солнечной активности и основана на том, что электронная плотность в F-области индийской зоны коррелирует с солнечным потоком  $F10.7$  см для каждого момента местного времени и каждого месяца. Используя эту характеристику, мы описываем модель электронной плотности. В этой модели мы использовали подбор методом наименьших квадратов и подбор многочлена. Электронная плотность, измеренная анализатором тормозящего потенциала (RPA) на спутнике SROSS C2 с 1995 по 2000 гг. и на спутнике FORMOSAT-1 (ROCSAT-1), находящимся в ведении Национальной организации космических исследований (NSPO, в настоящее время Тайваньское управление космических исследований (TASA)), Китай, Тайвань, с 1999 по 2004 г., использовалась для определения соотношения между  $N_e$  и  $F10.7$ . Средние высоты SROSS-C2 и FORMOSAT-1 составляют 500 км и 600 км соответственно. Из-за этой разницы высот наблюдаемые данные, полученные FORMOSAT-1, нормализуются таким образом, чтобы они совпадали с данными SROSS-C2. Мы сравнили данные, полученные с помощью модели, с наблюдениями и выяснили, что они хорошо согласуются. Данная модель может применяться к спокойным условиям ( $A_p < 15$ ) и ограничена фиксированной высотой 500 км в диапазоне широт от  $10^\circ$  S до  $10^\circ$  N вблизи меридиана  $75^\circ$  E.

**Ключевые слова:** экваториальная ионосфера; моделирование; цикл солнечной активности; математические и численные методы.

## INTRODUCTION

In order to illustrate the properties of the ionosphere and improve prediction capabilities, empirical models of electron density, electron temperature, ion temperature, critical frequency of F2 layer ( $f_oF2$ ), peak height of F2

layer ( $h_mF2$ ), etc. are very important. A large number of station-specific, regional, and global models of ionosphere based on in-situ measurements, incoherent scatter radar (ISR) measurements, middle and upper atmosphere (MU) radar measurements, etc. have been devel-

oped. An excellent review of many available empirical models has been presented by Bilitza [2002] (see also references therein). Among those models are the International Reference Ionosphere (IRI) [Bilitza, 1990, 2001], which was developed and periodically uploaded, and the International Union of Radio Science (URSI), which is the most widely used model. One empirical model providing the electron density profile is the  $N_e$  Quick model [Radicella, Zhang, 1995; Radicella, Leitinger, 2001; Leitinger et al., 2005]. Empirical models created using Incoherent Scatter Radar data are Millstone Hill (42.6° N, 288.5° W) [Holt et al., 2002] in the United States, Saint Santin [Zhang et al., 2004] in France (44.6° N, 2.2° E), Shigaraki (the MU radar site) [Zhang et al., 2007] in Japan (34.8° N, 136.1° E), Arecibo (18.3° N, 66.7° W) [Zhang et al., 2007] in Puerto Rico.

Ionization and peak density as represented by ionospheric total electron content (TEC) and  $N_mF2$  normally exhibits a linear relationship with solar activity measured in terms of the 10.7 cm solar flux index  $F10.7$  and the sunspot number  $R_z$ . However, there have been a number of reports which indicate that the linear relationship does not hold well near solar maximum, i.e. for very high values of  $F10.7$  [Titheridge, 1978; Bhuyan et al., 1983; Lakshmi et al., 1988; Kane, 1992; Rishbeth, 1993]. Balan et al. [1993, 1994] have shown that during intense solar cycle 21 when  $F10.7$  frequently exceeded 300 and reached a maximum value of 367, TEC and related  $F10.7$  increased nonlinearly. The observed nonlinear variation of ionization density with solar flux has been theoretically investigated by Balan et al. [1994] using the Sheffield University Plasmasphere Ionosphere model. The relative importance of neutral winds, neutral densities, and solar EUV fluxes in the observed nonlinear phenomenon has been explored. It has been found that the saturation of ionization is caused by the saturation of production of ionization due to the nonlinear increase in solar EUV fluxes while nonlinear increase in neutral density seems to have no effect on the saturation. In other words, the ionosphere (and atmosphere) responds linearly to solar EUV (or UV) inputs and  $F10.7$ . Using SROSS C2 and FORMOSAT-1 data, we have found a linear relationship between the electron density  $N_e$  and the  $F10.7$  cm solar flux from solar minimum to maximum of solar cycle 23. In this paper, we have derived a model of  $N_e$  for  $A_p < 15$  based on the best linear positive correlation between  $N_e$  and  $F10.7$ . We have used SROSS C2 data for the period 1995–2000 and FORMOSAT-1 data for the period 2001–2003 to derive this quiet day model. The model has been developed using all data in between  $\pm 10^\circ$  magnetic latitude for  $A_p < 15$  over the Indian subcontinent.

## DESCRIPTION OF THE MODEL

Using the best correlation between  $N_e$  and  $F10.7$ , we present a model of the electron density in this paper. In this model, we have used the least square fit and the polynomial fit. The model is a quiet day model ( $A_p < 15$ ), and it operated from 1995 to 2003 at an average altitude of 500 km. The latitude range of the model is  $10^\circ$  S to  $10^\circ$  N around the  $75^\circ$  E meridian. Since the average altitude of the satellite FORMOSAT-1 was 600 km, we have normalized the FORMOSAT-1  $N_e$  data to the alti-

tude to match it with the SROSS C2 data. For the period 1999–2000, we have both SROSS-C2 and FORMOSAT-1 data. In solar cycle 23, the  $F10.7$  cm flux varied from a minimum of 69 to a maximum of 237, and solar activity was not so intense. The yearly average  $F10.7$  values for 1999, 2000, 2001, 2002, 2003, and 2004 are approximately 143, 182, 185, 178, 129, and 107 respectively. Solar activity during the period 1999–2004 varies from moderate to slightly high levels. Therefore, for the period 1999–2000, we have calculated the electron density difference for an altitude difference of 100 km. This electron density difference was subtracted from the electron density obtained from the FORMOSAT-1 data at the peak of solar cycle 23.

The modeled density can be obtained from the following equation:

$$N_e = mf + c, \quad (1)$$

where  $f$  is the monthly mean  $F10.7$  cm solar flux,  $N_e$  is the monthly mean electron density for the current month;  $m$  and  $c$  are given by the following equations:

$$m = a_1 l^4 + a_2 l^3 + a_3 l^2 + a_4 l + a_5, \quad (2)$$

$$c = b_1 l^4 + b_2 l^3 + b_3 l^2 + b_4 l + b_5, \quad (3)$$

where  $l = 0, 1, 2, \dots, 23$  is the local time. Since we have found the polynomial fit as the best, we use the polynomial approximation in local time.

The coefficients  $a_1, a_2$ , and  $b_1, b_2$  are given in Table 1 for each of three seasons: summer, winter, and equinoxes. Coefficients are calculated for each season from monthly mean  $F10.7$ . We can calculate the modeled electron density for each month and for all levels of solar activity (low, medium, and high) over the Indian equatorial zone from monthly mean  $F10.7$ . For all summer months, the coefficient will be same, but monthly mean  $N_e$  for each local time is calculated from monthly mean  $F10.7$ . The same procedure is performed for the other seasons.

Table 1

Coefficients  $a_1, a_2$ , and  $b_1, b_2$ , for each of the three seasons: summer, winter, and equinoxes

|       | Summer                  | Winter                  | Equinoxes               |
|-------|-------------------------|-------------------------|-------------------------|
| $a_1$ | $0.0082 \cdot 10^8$     | $0.0072 \cdot 10^8$     | $0.0089 \cdot 10^8$     |
| $a_2$ | $-0.4518 \cdot 10^8$    | $-0.3949 \cdot 10^8$    | $-0.4933 \cdot 10^8$    |
| $a_3$ | $7.4041 \cdot 10^8$     | $6.5785 \cdot 10^8$     | $8.3164 \cdot 10^8$     |
| $a_4$ | $-31.299 \cdot 10^8$    | $-29.429 \cdot 10^8$    | $-38.353 \cdot 10^8$    |
| $a_5$ | $42.719 \cdot 10^8$     | $54.987 \cdot 10^8$     | $63.024 \cdot 10^8$     |
| $b_1$ | $0.0036 \cdot 10^{10}$  | $0.0047 \cdot 10^{10}$  | $0.003 \cdot 10^{10}$   |
| $b_2$ | $-0.2184 \cdot 10^{10}$ | $-0.2406 \cdot 10^{10}$ | $-0.1819 \cdot 10^{10}$ |
| $b_3$ | $3.9022 \cdot 10^{10}$  | $3.7718 \cdot 10^{10}$  | $3.3411 \cdot 10^{10}$  |
| $b_4$ | $-17.859 \cdot 10^{10}$ | $16.097 \cdot 10^{10}$  | $-16.68 \cdot 10^{10}$  |

## MODEL RESULTS AND VERIFICATIONS

Figure 1 shows superimposed plots of modeled and observed (SROSS-C2 and FORMOSAT-1) electron densities as function of local time for June, December, March, and September for three levels of solar activity: low (left panel), moderate (middle panel), and high (right panel). The daytime electron density starts increasing after sunrise becomes maximum at 12:00–15:00 hrs. The observed and modeled electron densities at noon are listed in Table 2 for comparison. The nighttime

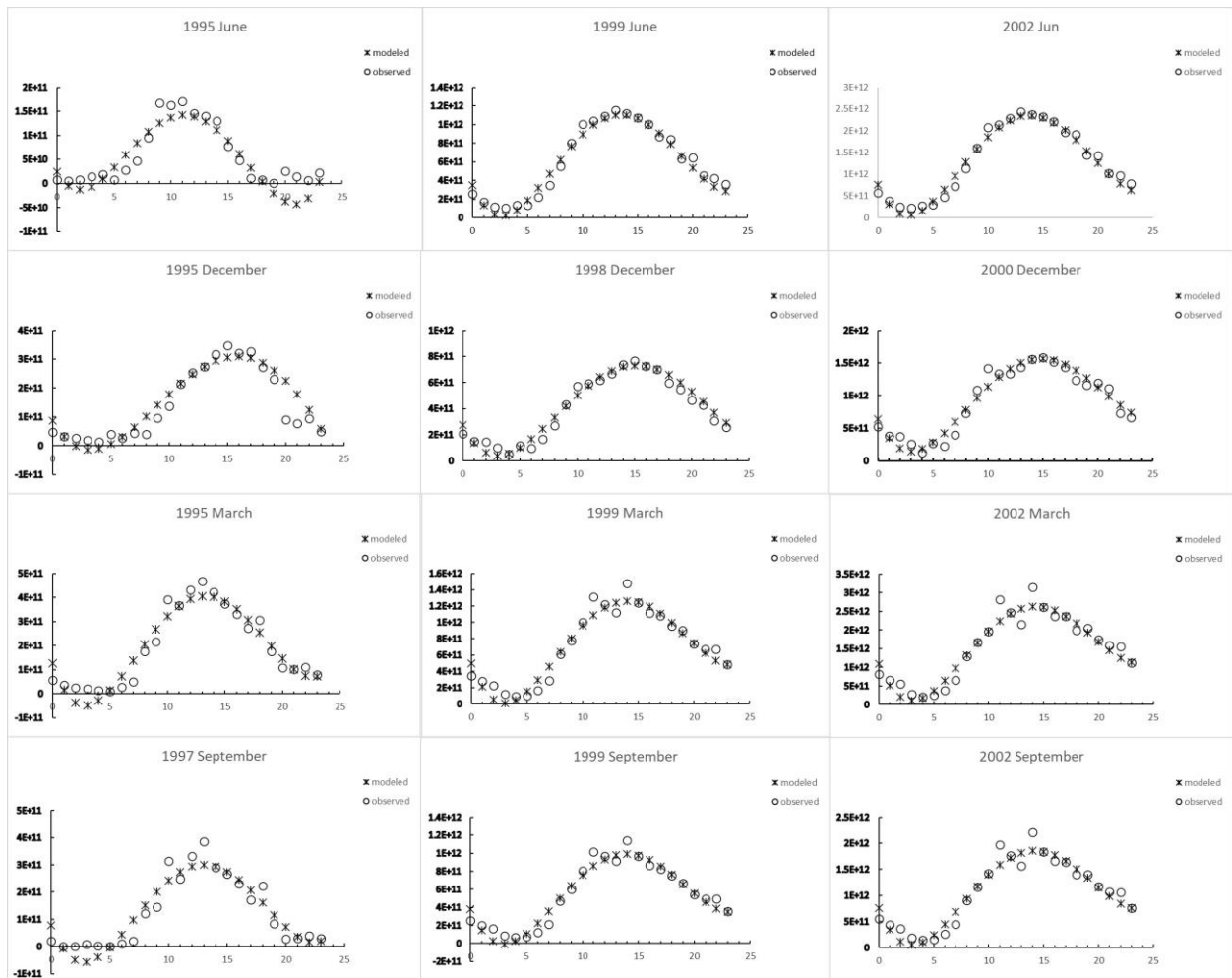


Fig. 1. Superimposed plots of modeled and observed electron densities as function of local time for low (left panel), moderate (middle panel), and high (right panel) solar activity

Table 2

Observed and modeled electron densities at noon

| Months   | Low solar activity   |                      | Moderate solar activity |                      | High solar activity  |                      |
|----------|----------------------|----------------------|-------------------------|----------------------|----------------------|----------------------|
|          | observed             | modeled              | observed                | modeled              | observed             | modeled              |
| June     | $1.45 \cdot 10^{11}$ | $1.39 \cdot 10^{11}$ | $1.09 \cdot 10^{12}$    | $1.06 \cdot 10^{12}$ | $2.29 \cdot 10^{12}$ | $2.24 \cdot 10^{12}$ |
| December | $2.53 \cdot 10^{11}$ | $2.53 \cdot 10^{11}$ | $5.94 \cdot 10^{11}$    | $5.78 \cdot 10^{11}$ | $1.34 \cdot 10^{12}$ | $1.41 \cdot 10^{12}$ |
| March    | $4.31 \cdot 10^{11}$ | $3.93 \cdot 10^{11}$ | $1.22 \cdot 10^{12}$    | $1.18 \cdot 10^{12}$ | $2.46 \cdot 10^{12}$ | $2.43 \cdot 10^{12}$ |

electron density is underestimated by the model for all levels of solar activity and all seasons. For low solar activity, the model gives negative electron density values for nighttime. Table 3 shows the observed and modeled values at 02:00 hr for comparison. Since this model is a regional model for the Indian region at the altitude of 500 km, the modelled data could not be compared with the electron density obtained from other satellites such as ISR or SWARM as they cannot provide  $N_e$  for all local times over the Indian zone. Therefore, the model presented in this paper cannot be compared with observations from other satellites.

### DISCUSSION

The regional and global empirical models of the ionosphere that have been developed so far across the world

are based on various mathematical and numerical techniques. The St. Santin incoherent scatter radar models [Zhang et al., 2004] and the Millstone Hill ISR models [Holt et al., 2002] have been created using a bin-fit technique. Liu et al. [2008] have designed an empirical model for the ionospheric propagation factor  $M(3000)F_2$  based on the empirical orthogonal function analysis method. Jain et al. [1996], Bhuyan and Baruah [1996], Unnikrishnan et al. [2002] have applied the harmonic analysis to regional empirical modeling of the ionospheric electron content (IEC) over Luning ( $25^\circ N$  and  $121.2^\circ E$ ),  $f_oF_2$  over India, and TEC over Palehua respectively. Oyama et al. [2004] have developed an empirical model for electron temperature, using measurements on board the Hinotori satellite; the model is based on spline-approximation of measured electron temperature  $T_e$  in 5-dimensional space comprised of solar activity

Table 3

Observed and modeled electron densities at 02:00 hr

| Months    | Low solar activity   |                       | Moderate solar activity |                      | High solar activity  |                      |
|-----------|----------------------|-----------------------|-------------------------|----------------------|----------------------|----------------------|
|           | observed             | modeled               | observed                | modeled              | observed             | modeled              |
| June      | $7.61 \cdot 10^9$    | $-1.30 \cdot 10^{10}$ | $1.14 \cdot 10^{11}$    | $3.42 \cdot 10^{10}$ | $2.50 \cdot 10^{11}$ | $2.94 \cdot 10^{11}$ |
| December  | $2.74 \cdot 10^{10}$ | $-1.41 \cdot 10^{10}$ | $1.45 \cdot 10^{11}$    | $6.45 \cdot 10^{10}$ | $3.76 \cdot 10^{11}$ | $1.93 \cdot 10^{11}$ |
| March     | $2.56 \cdot 10^{10}$ | $-3.82 \cdot 10^{10}$ | $2.28 \cdot 10^{11}$    | $2.56 \cdot 10^{11}$ | $5.50 \cdot 10^{11}$ | $2.05 \cdot 10^{11}$ |
| September | 1.4                  | $-4.99 \cdot 10^{10}$ | $1.64 \cdot 10^{11}$    | $2.61 \cdot 10^{10}$ | $3.68 \cdot 10^{11}$ | $1.21 \cdot 10^{11}$ |

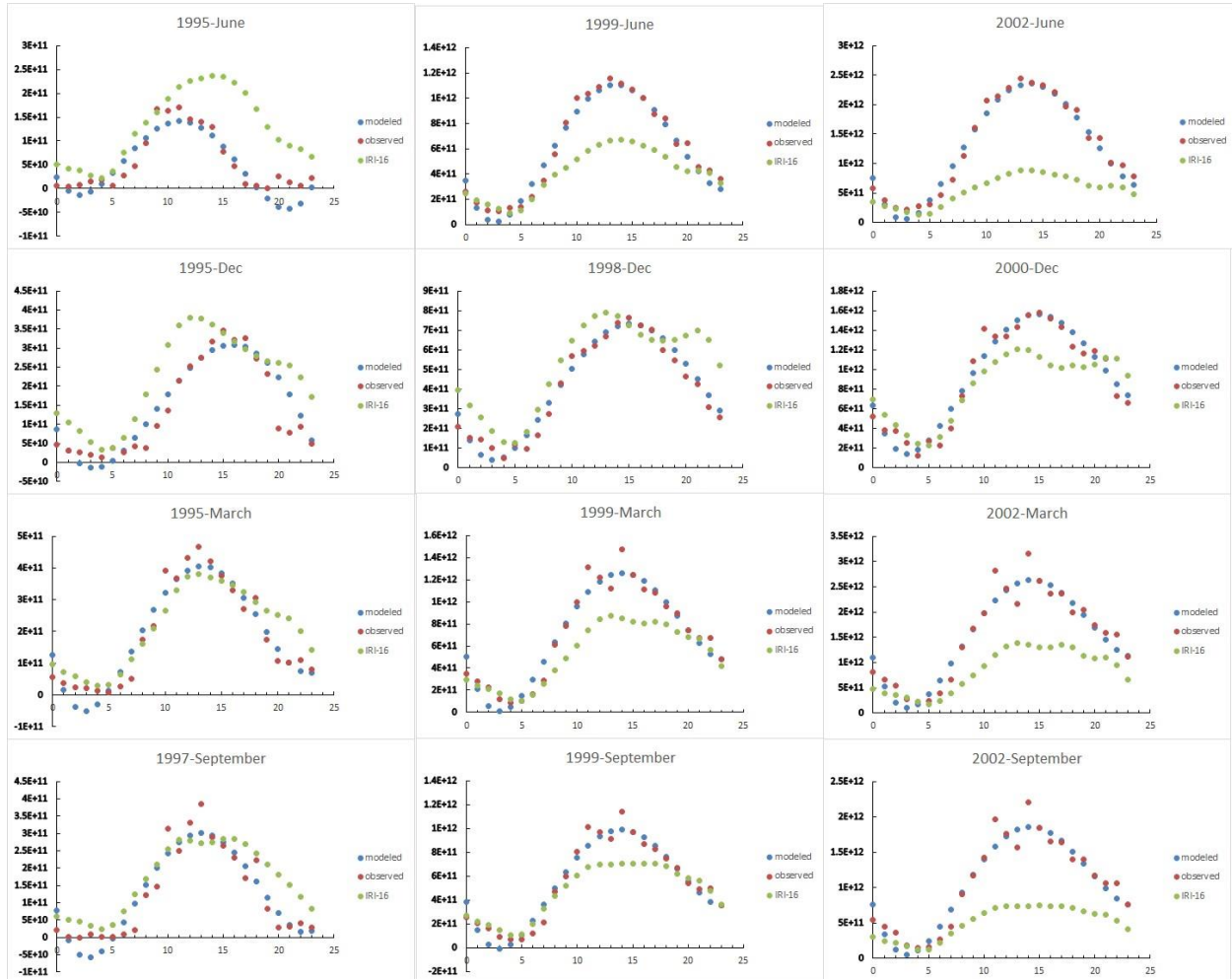


Fig. 2. Comparison of the observed and modeled data with IRI-16 (International Reference Ionosphere-16) model for low (left panel), moderate (middle panel) and high (right panel) solar activity

$F_{10.7}$ , month of the year, local time, geographic longitude, and geomagnetic latitude. Bhuyan and Chamua [2006] have presented an empirical model of  $T_e$  for the Indian equatorial and low latitudes using SROSS C2 RPA measurements; it is based on the regression analysis.

In this paper, we present a quiet day empirical model of electron density over the Indian zone, using the least square fit and the polynomial fit technique. Comparison between the model and the observed data shows that the model reproduces most of the features seen in measured electron density. For example, the daytime peak density occurs around 13:00 hr in summer and equinoxes, while in winter the peak density occurs two hours later at ~15:00 hr. However, the nighttime modeled electron densities are very low compared to the observed  $N_e$  during low solar activity for all seasons.

Figure 2 compares the observed and modeled data with IRI-16 (International Reference Ionosphere-16) model for all the three levels of solar activity, for summer, winter, and equinox months. From the figure it is seen that during low solar activity except for the equinox months and daytime (10:00–15:00 hrs) IRI overestimates observed and modeled electron densities for all local times. For moderate solar activity except for the winter month, the daytime electron density is underestimated by IRI for summer and equinox months. At 14:00 hr, IRI underestimates observed and modeled  $N_e$  by about 40 % in June, by about 43 % in March, and by about 38 % in September. During high solar activity, the daytime electron density is underestimated by IRI for summer, winter, and equinox months, whereas during nighttime IRI underestimates

$N_e$  for summer and equinox months, but overestimates it in the winter month.

At 14:00 hr, IRI underestimates  $N_e$  by about 28 % in December, by 62 % in June, by 57 % in March, and by 66 % in September. In December,  $N_e$  predicted by IRI-16 shows an evening enhancement for low, medium, and high solar activity. Also in December, the daytime maximum density occurs around 15:00 hr in case of observed and modeled data, whereas IRI predicts daytime maximum density around 13:00 hr.

## CONCLUSION

The electron density measured at ~500 km by the SROSS C2 satellite from 1995 to 2000 and at ~600 km by the FORMOSAT-1 satellite from 2001 to 2004 is used to derive an empirical model of electron density applicable to the Indian equatorial and low-latitude regions. It is based on the observation that the electron density in the F-region of the Indian equatorial and low-latitude ionosphere has positive correlation with the  $F_{10.7}$  cm solar flux.

The empirical model described in this paper is successful in reproducing the daytime electron densities for all season and all levels of solar activity. However, the nighttime electron density is underestimated by the model for all levels of solar activity and for all months. The drawback of the model is that it gives negative electron density values for low solar activity at nighttime.

Except for the equinox months, the IRI overestimates observed and modeled electron densities for all local times for low solar activity. During moderate solar activity, IRI underestimates the observed and modeled daytime electron densities in June, March, and September and overestimates them in December. At high solar activity, the daytime electron density is underestimated by IRI for all the four months, i. e. June, December, March, and September. IRI overestimates the nighttime electron density in December and underestimates it in June, March, and September. Bhuyan et al. [2003] have reported that IRI overestimates  $N_e$  at nearly all local times and in all seasons for low solar activity.

This model can be used as a regional alternative for electron density for almost full solar cycle. Nonetheless, the model has some limitations. It is limited to the fixed altitude of 500 km within the latitude range of 10° N to 10° S around the 75° E meridian and is applicable to quiet conditions ( $A_p < 15$ ). Since the International Reference Ionosphere cannot correctly predict  $N_e$  over the Indian subcontinent, the empirical model described in this paper can be incorporated in IRI for accurate prediction of the electron density over this region. This model can be helpful in developing an ionospheric map over the Indian subcontinent with the aid of other available resources such as the International Reference Ionosphere (IRI) model, other observed data over the region at different altitudes. The ionospheric map depicting accurate values of  $h_mF_2$  and  $f_oF_2$  along with the electron density profile at any location over the Indian subcontinent will be a useful tool for high frequency (HF) communications and space weather applications.

Authors wish to express their sincere thanks to the National Space Organization (NSPO) for the FORMOSAT-1 data.

## REFERENCES

- Balan N., Bailey G.J., Jayachandran B. Ionospheric evidence for a non-linear relationship between the solar EUV and 10.7 cm fluxes during an intense solar cycle. *Planet. Space Sci.* 1993, vol. 41, pp. 141–145. DOI: [10.1016/0032-0633\(93\)90043-2](https://doi.org/10.1016/0032-0633(93)90043-2).
- Balan N., Bailey G.J., Jenkins B., Rao P.B., Moffett R.J. Variations of ionospheric ionization and related solar fluxes during an intense solar cycle. *J. Geophys. Res.* 1994, vol. 99, pp. 2243–2253. DOI: [10.1029/93JA02099](https://doi.org/10.1029/93JA02099).
- Bhuyan P.K., Baruah S. A regional mapping of the  $f_oF_2$  over India as an additional input to IRI. *Adv. Space Res.* 1996, vol. 18, no. 6, pp. 205–208. DOI: [10.1016/0273-1177\(95\)00924-8](https://doi.org/10.1016/0273-1177(95)00924-8).
- Bhuyan P.K., Chamua M. An empirical model of electron temperature in the Indian topside ionosphere for solar minimum based on SROSS C2 RPA data. *Adv. Space Res.* 2006, vol. 37, pp. 897–902. DOI: [10.1016/j.asr.2005.09.016](https://doi.org/10.1016/j.asr.2005.09.016).
- Bhuyan P.K., Tyagi T.R., Singh L., Somayajulu Y.V. Ionospheric electron content measurements at a northern low midlatitude station through half a solar cycle. *J. Radio and Space Phys.* 1983, vol. 12, pp. 84–93.
- Bhuyan P.K., Chamua M., Bhuyan K., Subrahmanyam P., Garg S.C. Diurnal, seasonal and latitudinal variation of electron density in the topside F-region of the Indian zone ionosphere at solar minimum and comparison with the IRI. *J. Atmos. Solar-Terr. Phys.* 2003, vol. 65, iss.3, pp. 359–368. DOI: [10.1016/S1364-6826\(02\)00294-8](https://doi.org/10.1016/S1364-6826(02)00294-8).
- Bilitza D. International Reference Ionosphere. Rep. NSSDC/WDC-R&S 90-22. *World Data for Rockets and Satellites*. National Space Science Data Centre. Greenbelt, Md. 1990.
- Bilitza D. International Reference Ionosphere 2000. *Radio Sci.* 2001, vol. 36, iss. 2, pp. 261–275. DOI: [10.1029/2000RS002432](https://doi.org/10.1029/2000RS002432).
- Bilitza D. Ionospheric models for radio propagation studies. *Rev. Radio Sci. 1999–2002*, edited by W.R. Stone, IEEE and Wiley. 2002, pp. 625–679.
- Holt J.M., Zhang S.-R., Buonsanto M.J. Regional and local ionospheric models based on Millstone Hill incoherent scatter radar data. *Geophys. Res. Lett.* 2002, vol. 29, no. 8. DOI: [10.1029/2002GL014678](https://doi.org/10.1029/2002GL014678).
- Jain S., Vijay S.K., Gwal A.K. An empirical model for IEC over Luning. *Adv. Space Res.* 1996, vol. 18, no. 6, pp. 263–266. DOI: [10.1016/0273-1177\(95\)00935-3](https://doi.org/10.1016/0273-1177(95)00935-3).
- Kane K.P. Solar cycle variation of  $f_oF_2$ . *J. Atmos. Terr. Phys.* 1992, vol. 54, pp. 1201–1218. DOI: [10.1016/0021-9169\(92\)90145-B](https://doi.org/10.1016/0021-9169(92)90145-B).
- Lakshmi D.R., Reddy B.M., Dabas R.S. On the possible use of recent EUV data for ionospheric predictions. *J. Atmos. Terr. Phys.* 1988, vol. 50, no. 3, pp. 207–213. DOI: [10.1016/0021-9169\(88\)90069-4](https://doi.org/10.1016/0021-9169(88)90069-4).
- Leitinger R., Zhang M.L., Radicella S.M. An improved bottomside for the ionospheric electron density model Ne-Quick. *Ann. Geophys.* 2005, vol. 48, no. 3, pp. 525–534. DOI: [10.4401/ag-3217](https://doi.org/10.4401/ag-3217).
- Liu C., Zhang M.-L., Wan W., Liu L., Ning B. Modeling M (3000) F2 based on empirical orthogonal function analysis method. *Radio Sci.* 2008, vol. 43, RS1003. DOI: [10.1029/2007RS003694](https://doi.org/10.1029/2007RS003694).
- Oyama K.-I., Marinov P., Kutiev I., Watanabe S. Low latitude model of  $T_e$  at 600 km based on Hinotori satellite data. *Adv. Space Res.* 2004, vol. 34, pp. 2004–2009. DOI: [10.1016/j.asr.2004.07.013](https://doi.org/10.1016/j.asr.2004.07.013).
- Radicella S.M., Zhang M.L., The improved DGR analytical model of electron density height profile and total electron content in the ionosphere. *Ann. Geophys.* 1995, vol. 38 (1), pp. 35–41. DOI: [10.4401/ag-4130](https://doi.org/10.4401/ag-4130).
- Radicella S.M., Leitinger R. The evolution of the DGR approach to model electron density profiles. *Adv. Space Res.* 2001, vol. 27, no. 1, pp. 35–40. DOI: [10.1016/S0273-1177\(00\)00138-1](https://doi.org/10.1016/S0273-1177(00)00138-1).

Rishbeth H. Day-to-day ionospheric variations in a period of high solar activity. *J. Atmos. Terr. Phys.* 1993, vol. 55,iss. 2, pp. 165–171. DOI: [10.1016/0021-9169\(93\)90121-E](https://doi.org/10.1016/0021-9169(93)90121-E).

Titheridge J.E. The electron content of the southern mid-latitude ionosphere, 1965–1971. *J. Atmos. Terr. Phys.* 1978, vol. 35, iss. 5, pp. 981–1001. DOI: [10.1016/0021-9169\(73\)90077-9](https://doi.org/10.1016/0021-9169(73)90077-9).

Unnikrishnan K., Nair R.B., Venugopal C. Harmonic analysis and an empirical model for TEC over Palehua. *J. Atmos. Solar-Terr. Phys.* 2002, vol. 64, no. 17, pp. 1833–1840. DOI: [10.1016/S1364-6826\(02\)00187-6](https://doi.org/10.1016/S1364-6826(02)00187-6).

Zhang S.-R., Holt J.M., Zaluca A.M. Midlatitude ionospheric plasma temperature climatology and empirical model based on Saint Santin incoherent scatter radar data from 1966 to 1987. *J. Geophys. Res. Lett.* 2004, vol. 109, A11311. DOI: [10.1029/2004JA010709](https://doi.org/10.1029/2004JA010709).

Zhang S.-R., John M.H., Bilitza D.K., Eyken T.V., Mc Geady M., Amory-Mazaudier C., Fukao S., Sulzer M. Multiple-site comparisons between models of incoherent scatter radar and IRI. *Adv. Space Res.* 2007, vol. 39, no. 5, pp. 910–917. DOI: [10.1016/j.asr.2006.05.027](https://doi.org/10.1016/j.asr.2006.05.027).

*How to cite this article:*

Chamua M., Bhuyan P.K., Bhuyan K. A quiet day empirical model of electron density in the Indian equatorial F-region. *Solnechno-Zemnaya Fizika*. 2023. Vol. 9, iss. 1. P. 73–78. DOI: [10.12737/szf-91202308](https://doi.org/10.12737/szf-91202308).